# Interpretation of scaling properties of electroencephalographic fluctuations via spectral analysis and underlying physiology

P. A. Robinson

*School of Physics, University of Sydney, New South Wales 2006, Australia*
*and Brain Dynamics Center, Westmead Hospital and University of Sydney, Westmead, New South Wales 2145, Australia*

Detrended fluctuation analysis has recently demonstrated the existence of two approximate temporal scaling regimes in locally detrended human electroencephalographic (EEG) fluctuations, and has suggested a connection between the location of the breakpoint between regimes and the alpha resonance near 10 Hz. It is shown here that these scalings can be explained in terms of the filtering of the underlying power spectrum implied by the detrending process. Using a recent physiologically based model of EEG generation, the main features of the scalings, and deviations from them, are related to the underlying physiology of dendritic propagation and muscle electrical activity, and it is concluded that the effects of such physiological features are usually clearer in spectra.

## I. INTRODUCTION

Electroencephalographic (EEG) measurements are widely used to probe brain dynamics [1,2], but have traditionally been analyzed only qualitatively, or via phenomenological measures [3]. In recent years, numerous tools have been used to quantify EEGs from a signal-analysis perspective, most recently via detrended fluctuation analysis (DFA) [4–6] of scaling properties of root-mean-square fluctuations with respect to detrended EEG time series [7,8]. This numerical analysis revealed two temporal scaling regimes of EEG fluctuations, separated by a breakpoint near 0.1 s. The scaling exponents in these regimes were found to be quite variable, with potential implications for the classification of EEGs into subtypes [7].

This paper examines EEG scaling properties from two perspectives. The first part of the analysis shows that the scaling properties can be derived from generic properties of the EEG power spectrum, and that the asymptotic exponents of the DFA temporal scalings are universal. The scaling properties are shown to arise from a weighted integral over the power spectrum, with the weighting corresponding to the filtering implicit in the detrending process. In the second part of the analysis, it is noted that, superposed on the asymptotic scalings are variations that correspond to structure in the power spectrum. These are interpreted in terms of the underlying physiology using a recent theory of EEG generation that has been found to yield excellent agreement with observations of EEG spectra [9], evoked response potentials [10], and other phenomena [11]. The breakpoint between scalings is shown to be related to dendritic time constants, rather than the alpha frequency, as was originally asserted [7]. Indeed, because of the averaging implicit in DFA, the main effects arise from gross changes in spectral shape, rather than from narrow peaks like alpha. Changes in spectral slope and electromyographic (EMG, due to muscular electrical activity) contributions are consistent with observed departures from the asymptotic scaling exponents in the regime investigated in Ref. [7], and with the resulting variation in numerically determined values.

## II. THEORY

### A. Scaling properties

Denoting the EEG time series by $\phi(t)$, detrended fluctuation analysis proceeds by dividing the whole time series into windows of length $T$. In each of these windows, centered at $T_0$ for example, the best linear least-squares fit $\tilde{\phi}(t;T,T_0)$ is computed. The mean square deviation $F^2(T)$ between $\phi(t)$ and the best linear least-squares fit is then calculated as a function of $T$, after averaging over $T_0$ [7]. This gives

$$F^2(T) = \left\langle \frac{1}{T} \int_{T_0 - T/2}^{T_0 + T/2} [\phi(t) - \tilde{\phi}(t;T,T_0)]^2 dt \right\rangle, \quad (1)$$

where the angular brackets denote the average over $T_0$.

The quantity $F(T)$ has been found to have two scaling regimes: a roughly power-law increase at small $T$, followed by a flattening at $T \gtrsim 0.1$ s [7].

### B. Analysis via the power spectrum

It is straightforward to calculate $F(T)$ via integrals over the power spectrum. If we use a bar to denote the average of a quantity over an interval of length $T$, centered at $T_0$, then the best linear least-squares fit is

$$\tilde{\phi}(t;T,T_0) = a + bt', \quad (2)$$

$$a = \bar{\phi}, \quad (3)$$

$$b = \overline{t'\phi}/\overline{t'^2}, \quad (4)$$

$$= 12\overline{t'\phi}/T^2, \quad (5)$$

with $t' = t - T_0$. We then find

$$F^2(T) = \langle \overline{\phi^2} - \bar{\phi}^2 - 12(\overline{t'\phi})^2/T^2 \rangle, \quad (6)$$

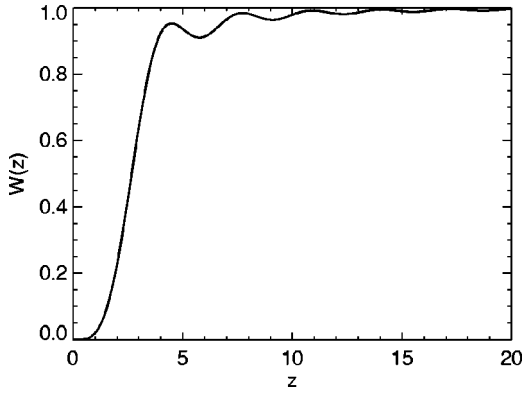where we have noted that $\langle \overline{\phi^2} \rangle = \langle \phi^2 \rangle$.

FIG. 1. Weight function $W(z)$ vs $z$, with $z = \omega T/2$.

The terms in Eq. (6) can be evaluated by replacing $\phi(t)$ by its Fourier representation in the average over $T$ and exchanging the order of integration before averaging over $T_0$. This gives

$$\bar{\phi} = \int \frac{d\omega}{2\pi} \phi(\omega) e^{-i\omega T_0} \mathrm{sinc}(\omega T/2), \qquad (7)$$

with $\mathrm{sinc}(x) = \sin(x)/x$, and where the bounds of integration are $\pm\infty$. Hence,

$$\langle(\bar{\phi})^2\rangle = \int \frac{d\omega}{2\pi} |\phi(\omega)|^2 \mathrm{sinc}^2(\omega T/2), \qquad (8)$$

which is simply a weighted integral over the power spectrum of $\phi$. A similar calculation yields

$$\langle(\overline{t'\phi})^2\rangle = \int \frac{d\omega}{2\pi} |\phi(\omega)|^2 \left[ \frac{d\,\mathrm{sinc}(\omega T/2)}{d\omega} \right]^2, \qquad (9)$$

$$\langle \phi^2 \rangle = \int \frac{d\omega}{2\pi} |\phi(\omega)|^2, \qquad (10)$$

the last result simply being a statement of Parseval's theorem. Overall, we thus find

$$F^2(T) = \int \frac{d\omega}{2\pi} |\phi(\omega)|^2 \left[ 1 - \mathrm{sinc}^2(\omega T/2) \right.$$
$$\left. -3 \left\{ \frac{d\,\mathrm{sinc}(\omega T/2)}{d(\omega T/2)} \right\}^2 \right]. \qquad (11)$$

The form of the weight function $W(\omega T/2)$ in the square brackets in Eq. (11) is shown in Fig. 1. It has an approximately quartic form for $\omega \lesssim 8/T$, with small and diminishing oscillations just below unity thereafter. The scaling properties of $F(T)$ thus depend on whether the power spectrum $|\phi(\omega)|^2$ is concentrated in the quartic regime of $W$, or significantly overlaps the near-constant regime. If the power spectrum is concentrated at $|\omega| \lesssim \omega_c$, where $\omega_c$ denotes a characteristic upper bound in frequency, then two regimes exist:

$$F(T) = T^2 [\langle (d^2\phi/dt^2)^2 \rangle / 720]^{1/2}, \qquad (12)$$

$$F(T) = \langle \phi^2 \rangle^{1/2} = \mathrm{const}, \qquad (13)$$

for $T \lesssim 8/\omega_c$ and $T \gtrsim 8/\omega_c$, respectively. The exponents of these asymptotic $T$ dependences are universal, provided the integral in Eq. (11) converges, as it must for any physical system. However, departures can occur over substantial ranges if there is a $1/\omega^a$ dependence (with $a$ constant) at low (but nonzero) frequencies, or a slow power-law falloff in the power spectrum at high frequencies.

A previous analysis showed that the DFA curve tends to flatten at large $T$, with a scaling exponent that was typically small (usually $<0.1$ and always $<0.5$), but somewhat uncertain owing to the relatively small range of scales over which it was determined experimentally [7]. The small-$T$ scaling exponent was found to be more strongly variable, and more uncertain, with values scattered between roughly 0.2 and 1.5, and a mean slightly below 1. However, examination of Fig. 2 of Ref. [4] shows that the slope varies significantly with $T$ in each dataset, with signs of steepening at the smallest $T$. As we will see below, the deviations from the mean behavior that appear to cause much of the scatter in the numerically determined exponents [7] arise from gross features in the power spectrum that are sufficiently broadband to strongly affect the behavior of the integral.

### C. Analysis via neurophysical modeling

We recently developed a physiologically based model of EEG generation that predicts the power spectrum from quantities such as corticothalamic connectivities, synaptic strengths, dendritic time constants, neural conduction speeds, axonal ranges, and the effects of the EMG artifact [9–13]. These predictions have succeeded in reproducing spectra in a variety of brain states, and the model also reproduces a variety of other EEG phenomena [9–11,13]. The details of the model are given in the references just cited, so we do not repeat them here. The theoretical expression for the scalp spectrum is

$$P(\omega) = P_{EEG}(\omega) + P_{EMG}(\omega), \qquad (14)$$

$$P_{EEG}(\omega) = P_0 \left| \frac{L^2}{(1 - G_{ei}L)(1 - G_{srs}L^2)} \right|^2 \frac{\theta}{q^2 r_e^2 \sin\theta}, \qquad (15)$$

$$P_{EMG}(\omega) = \frac{A(\omega/\omega_{EMG})^2}{(1 + \omega^2/\omega_{EMG}^2)^2}, \qquad (16)$$

where

$$q^2 r_e^2 = (1 - i\omega/\gamma_e)^2 + \frac{1}{1 - G_{ei}L}$$
$$\times \left[ G_{ee}L + \frac{(G_{ese}L^2 + G_{esre}L^3)e^{i\omega t_0}}{1 - G_{srs}L^2} \right], \qquad (17)$$

$$L(\omega) = (1 - i\omega/\alpha)^{-1}(1 - i\omega/\beta)^{-1}, \qquad (18)$$
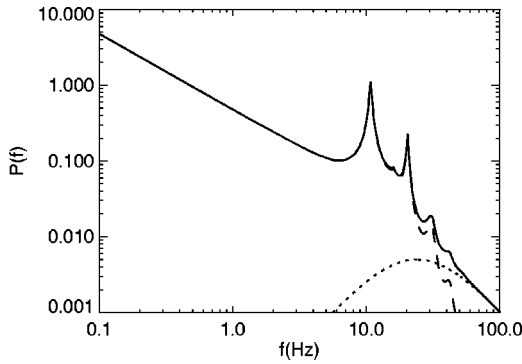
FIG. 2. Illustrative spectra from a physiologically based EEG model, for the parameters in the text, with EMG activity (solid curve) and without EMG activity (dashed curve). The EMG spectrum is also shown (dotted curve).

$\theta$ is the complex argument of $q^2$, $t_0 \approx 80$ ms is the time taken for signals to travel from the cortex to the thalamus and back, $\alpha \approx 60$ s$^{-1}$ and $\beta \approx 4\alpha$ are dendritic rate constants, $\gamma_e \approx 120$ s$^{-1}$ is a characteristic damping parameter of cortical signals, $r_e \approx 80$ mm is the characteristic excitatory axonal range, the $G$'s are gains for the transmission of signals involving various populations of neurons, with $G_{ee} \approx 4$, $G_{ei} \approx -6$, $G_{ese} \approx 9$, $G_{esre} \approx -5$, $G_{srs} \approx -1$, $A/P_0 \approx 0.02$, and $\omega_{EMG} \approx 150$ s$^{-1}$ is the characteristic EMG frequency; the parameter values are similar to those used in the papers cited in this section. The parameter $P_0$ is an overall normalization, which is not relevant here and is set to unity for simplicity. The effects of volume conduction are neglected in Eq. (14)–(18) as they are not essential for the illustrative purposes required here; however, volume conduction attenuates high-wave-number (and, hence, high-frequency, via the EEG wave dispersion relation) parts of the EEG spectrum, but not the EMG spectrum. This strengthens the conclusions below.

Figure 2 shows illustrative spectra calculated from (14)–(18) for the above parameters, with and without the EMG activity. One key feature illustrated in Fig. 2 is that the model relates the alpha peak to the fundamental resonance of corticothalamic feedback loops, with a frequency $f_\alpha \approx 1/t_0 \approx 10$ Hz [9,11]. There is also a knee in the spectrum, due to low-pass dendritic filtering below a frequency $\approx (\alpha\beta)^{1/2}/(2\pi)$, corresponding to about 15 Hz for the above parameters [9,12]. EMG activity has a small peak relative to the EEG activity, and contributes only 5% of the total activity in this example.

Figure 3 shows the detrended fluctuation transforms of the two spectra in Fig. 2, computed via Eq. (11) with an upper bound at $\omega = 200\pi$ s$^{-1}$ to accord with the experimental filter settings [7]. In the pure EEG case, we see a rapid switchover between the scalings (12) and (13). Figure 4 shows that this occurs at a value of $T$ that varies approximately inversely with $\alpha$ (and, hence, with $\beta = 4\alpha$). In contrast, further numerical investigations show that there is hardly any variation with $t_0$, and that enhancing or suppressing the alpha peak also scarcely affects $F(T)$ because of the smearing effects of the integration in Eq. (11).

Figure 3 also shows the effects of EMG activity in a typical frequency range and at a level that is realistic, but some-
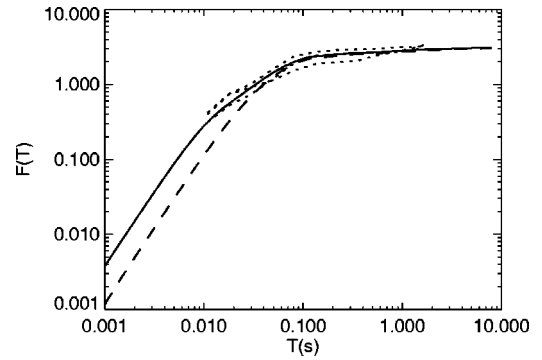


FIG. 3. Rms detrended fluctuation amplitude $F(T)$ vs $T$ for the EEG and total spectra in Fig. 2 (solid curve, with EMG activity; dashed, without EMG activity), compared with data from the three curves in Fig. 2 of Ref. [7] (dotted curves, renormalized to a common value).

what above what is ideally achievable [13]. EMG activity introduces a region of intermediate scaling with smaller exponents for $T$ in the tens of milliseconds, in accord with the data from Fig. 2 of Ref. [7], the trends in which are overplotted. Although the authors of Ref. [7] took precautions to eliminate head movements (which generate EMG activity in neck muscles), jaw and facial muscles can yield significant contributions unless the subjects are very carefully instructed to relax them, and succeed in doing so [13]. These contributions are also likely to vary with respect to the electrode, with minimal EMG activity near the crown of the head (the Cz electrode in the International 10-20 System), thus plausibly accounting for both the scalings observed in this range, and their relatively high interelectrode variability [7]. In the presence of significant EMG activity, the results here imply that larger exponents should be found near the crown of the head than at electrodes nearer ear level, for $T$ in the tens of milliseconds.

## III. CONCLUSION

In summary, detrended fluctuation analysis of EEG signals has been examined from a spectral viewpoint, and via physiologically based modeling. Asymptotic exponents are universal for any spectrum that has a sufficiently steep falloff
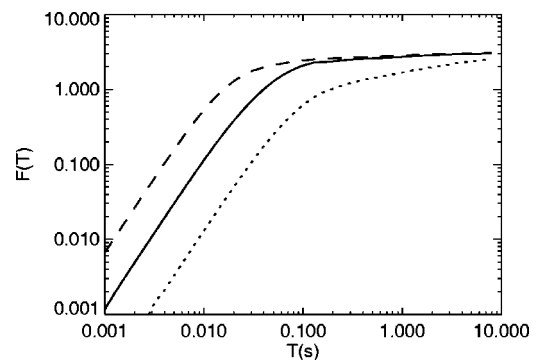


FIG. 4. $F(T)$ vs $T$ without EMG activity for the parameters of Fig. 2 apart from $\alpha = \beta/4 = 20, 60, 200$ s$^{-1}$ for the dotted, solid, and dashed curves, respectively.

at high frequencies to ensure convergence of the integral in Eq. (11). Intermediate-range exponents can differ from asymptotic values as a reflection of large scale features in the spectrum, whereas narrow spectral peaks have little effect. Hence, it is found that the main breakpoint in the scalings is related primarily to dendritic filtering, rather than the alpha frequency, as was previously suggested. Comparison with illustrative physiologically based spectra shows that small-$T$ departures from the asymptotic scalings are plausibly associated with the EMG muscle artifact, even when present at quite low amplitudes. This is due to the slower frequency falloff of EMG activity and its characteristically higher frequencies.

The overall conclusion is thus that DFA gives useful insights into physiological parameters, but that these tend to be less clear than in spectra, owing to the smearing effects of the integrations implicit in DFA. Large-$T$ fluctuations and corresponding marginal-stability scalings may also be probed via spectra of detrended time series, by ensuring that trend artifacts such as reference voltage drifts are minimized, or by magnetoencephalographic means that avoid such influences. In previous works, $1/f$ ranges evident in power spectra at low frequencies have been observed and related to system scaling behavior [13,14].

[1] N. Niedermeyer and F. H. Lopes da Silva, *Electroencephalography: Basic Principles, Clinical Applications, and Related Fields*, 4th ed. (Williams and Wilkins, Baltimore, 1999).

[2] P. L. Nunez, *Neocortical Dynamics and Human EEG Rhythms* (Oxford University, Oxford, 1995).

[3] *Quantitative EEG and Neurofeedback*, edited by J.R. Evans and A. Abarbanel (Academic, San Diego, 1999).

[4] S.V. Buldyrev, A.L. Goldberger, S. Havlin, C.-K. Peng, H.E. Stanley, M.H.R. Stanley, and M. Simons, Biophys. J. **65**, 2673 (1993).

[5] C.-K. Peng, S.V. Buldyrev, S. Havlin, M. Simons, H.E. Stanley, and A.L. Goldberger, Phys. Rev. E **49**, 1685 (1994).

[6] K. Hu, P.C. Ivanov, Z. Chen, P. Carpena, and H.E. Stanley, Phys. Rev. E **64**, 011114 (2001).

[7] R.C. Hwa and T.C. Ferree, Phys. Rev. E **66**, 021901 (2002).

[8] P.A. Watters, Complexity **5**, 1 (1998).

[9] P.A. Robinson, C.J. Rennie, J.J. Wright, H. Bahramali, E. Gordon, and D.L. Rowe, Phys. Rev. E **63**, 021903 (2001).

[10] C.J. Rennie, P.A. Robinson, and J.J. Wright, Biol. Cybern., **86**, 457 (2002).

[11] P.A. Robinson, C.J. Rennie, and D.L. Rowe, Phys. Rev. E **65**, 041924 (2002).

[12] P.A. Robinson, C.J. Rennie, and J.J. Wright, Phys. Rev. E **56**, 826 (1997).

[13] D.L. Rowe, P.A. Robinson, C.J. Rennie, and R.C. Powles (unpublished).

[14] E. Novikov, A. Novikov, D. Shannahoff-Khalsa, B. Schwartz, and J. Wright, Phys. Rev. E **56**, R2387 (1997).